

Scattering from Spatially Localized Chaotic and Disordered Systems

L.E. Reichl and G. Akguc

Center for Studies in Statistical Mechanics and Complex Systems
The University of Texas at Austin
Austin, Texas 78712

December 2, 2024

Abstract

A version of scattering theory that was developed many years ago to treat nuclear scattering processes, has provided a powerful tool to study universality in scattering processes involving open quantum systems with underlying classically chaotic dynamics. Recently, it has been used to make random matrix theory predictions concerning the statistical properties of scattering resonances in mesoscopic electron waveguides and electromagnetic waveguides. We provide a simple derivation of this scattering theory and we compare its predictions to those obtained from an exactly solvable scattering model; and we use it to study the scattering of a particle wave from a random potential. This method may prove useful in distinguishing the effects of chaos from the effects of disorder in real scattering processes.

1 Introduction

Interest in the dynamical properties of open quantum systems at mesoscopic and atomic scales has lead to a rebirth of a form of scattering theory which was originally developed to deal with very complicated nuclear collision processes. The origin of the scattering theory that we consider here came from the recognition that a collision between two nucleons, one of which is very heavy, can lead to the creation of an unstable, but very long-lived, compound nucleus which eventually decays. In the late 1930's, Kapur and Peierls [1] used this

fact to formulate a nonperturbative approach to scattering theory in which the compound nucleus was viewed as a stable object which was made unstable by weak coupling to the continuum. In the late 1940's, Wigner and Eisenbud [2] developed an alternate version of the the Kapur-Peierls theory which lead to the very widely used R-matrix approach to scattering theory [3]. The idea behind both these theories is to decompose configuration space into an internal region (reaction region) and an external asymptotic scattering region. As we shall see, this approach can be made clean and rigorous if there is an abrupt (in configuration space) transition between the scattering region and the asymptotic region. The internal region can be modeled in terms of a complete set of states with fixed boundary conditions on the surface of the internal region. The internal states can then be coupled to the external asymptotic states. Bloch [4] and Feshback [5] both showed that a consistent theory requires that the coupling between the internal and external regions must be singular. In the 1960's, Weidenmuller developed a phenomenological Hamiltonian approach to nuclear scattering based on this picture [6]. The Hamiltonian for the interior region was based on the shell model of the nucleus. The Hamiltonian for the exterior scattering region described the asymptotic states. The strength of the coupling between the interior and exterior regions was an unknown input parameter.

The Weidenmuller approach to scattering theory created a framework with which to study the manifestations of chaos in the scattering properties of nuclear systems, as well as mesoscopic and atomic systems. It is now well known that chaos manifests itself in bounded quantum systems by affecting the statistical distribution of spacings between energy levels [7]. For open quantum systems, in regimes where scattering resonances are not strongly overlapping, underlying chaos affects the statistical distribution of resonance spacings and resonance widths [8]. If the Hamiltonian of the interior region is chosen to be a random matrix Hamiltonian, then predictions can be made as to the statistical properties of resonance spacings and resonance widths. These predictions can

then be compared to nuclear scattering resonances, or to resonances in electron waveguides [[9]], [13], and [[11]] and electro-magnetic resonators [[10]] and [14] whose cavities have been constructed to yield classically chaotic behavior. The agreement between random matrix theory predictions and numerical and laboratory experiments is quite good.

The Weidenmuller Hamiltonian is phenomenological and does not have information about the strength of the interface coupling. The random matrix theories treat the interface coupling as an input parameter. In a real dynamical system, however, one needs a way to rigorously determine the coupling at the interface of the internal and external regions. A very useful way to fix the coupling at the interface was provided by Pavlov [12]. The idea of Pavlov was that the surface coupling could be fixed by the requirement that the total Hamiltonian (including interior and exterior regions) be Hermitian.

In this paper, we use a simple textbook scattering problem to illustrate and clarify many issues concerning this approach to scattering, and we then use it to study the effect of disorder on the scattering process.

In Section (2), we describe the “textbook” scattering problem and obtain exact expressions for the reaction function, the scattering function, and the Wigner delay times. In Section (3), we develop the Hamiltonian for interior and exterior regions of the scattering system. In Section (4) we derive the Hermiticity condition. In Section (5), we derive the reaction function. In Section (6), we derive the scattering function and locate resonance energies for the case of a smooth scattering potential. In Section (7), we use this theory to study the scattering of a particle wave from a random scattering potential. Finally, in Section (7), we make some concluding remarks.

2 Exact Solution

We will first consider the scattering of a particle of mass, m , due to the potential shown in Fig. (1). The quantum particle enters from the right with energy E and is reflected back to the left by an infinitely hard wall located at $x = 0$. A barrier of height, V_0 , is located $0 < x < a$. The Schroedinger equation, which describes propagation of a particle wave, $\Psi(x, t)$, for all times, t , is given by

$$i\hbar \frac{\partial \Psi(x, t)}{\partial t} = -\frac{\hbar^2}{2m} \frac{\partial^2 \Psi(x, t)}{\partial x^2} + V(x)\Psi(x, t), \quad (2.1)$$

where \hbar is Planck's constant and the potential, $V(x) = \infty$ for $(-\infty < x \leq 0)$, $V(x) = V_0$ for $(0 < x \leq a)$, and $V(x) = 0$ for $(a < x < \infty)$. Since the potential is infinite for $-\infty < x < 0$, no wavefunction can exist in that region of space.

The Schroedinger equation for energy eigenstates $\Phi_E^I(x)$, for Region I ($0 < x < a$) in Fig. (1), is

$$-\frac{\hbar^2}{2m} \frac{d^2 \Phi_E^I(x)}{dx^2} + V_0 \Phi_E^I(x) = E \Phi_E^I(x), \quad (2.1)$$

Energy eigenstates in Region I have the form

$$\Phi_E^I(x) = A \sin(k' x) \quad (2.2)$$

where $k' = \sqrt{\frac{2m}{\hbar^2}(E - V_0)}$ and A is a normalization constant. The Schroedinger equation for energy eigenstates $\Phi_E^{II}(x)$, for Region II ($a < x < -\infty$) in Fig. 1, is

$$-\frac{\hbar^2}{2m} \frac{d^2 \Phi_E^{II}(x)}{dx^2} = E \Phi_E^{II}(x), \quad (2.3)$$

Energy eigenstates in Region II have the form

$$\Phi_E^{II}(x) = B(e^{-ikx} - S(E)e^{ikx}), \quad (2.4)$$

where $k = \sqrt{\frac{2m}{\hbar^2}E}$. The first term describes the incoming part of the energy eigenstate and the second term describes the outgoing part of that state. The constant, B , is a normalization constant and $S(E)$ is the *scattering function*.

When $V_0 = 0$, then $S(E) = 1$ and the incoming wave is reflected from the wall at $x = 0$ with an overall phase shift of π since we can rewrite the minus sign as $e^{i\pi}$. Thus, $S(E)$, contains information about the phase shift of the scattered wave due to the potential barrier, V_0 , in the region, $0 < x < a$.

We can determine how the two parts of the energy eigenstate are connected by the condition that the wavefunction and the slope of the wavefunction must be continuous at $x = a$. These two conditions can be combined into a statement that the "logarithmic derivative" of the wavefunction must be continuous at the interface. Thus we must have

$$\frac{1}{R(E)} \equiv \frac{a}{\Phi_E^I(a)} \frac{d\Phi_E^I}{dx} \Big|_a = \frac{a}{\Phi_E^{II}(a)} \frac{d\Phi_E^{II}}{dx} \Big|_a \quad (2.5)$$

at the interface. The function, $R(E)$, is called the *reaction function* and it will play an important role in the following sections. The S-matrix is then given by

$$S(E) = e^{-2ika} \frac{(1 + ikaR(E))}{(1 - ikaR(E))}. \quad (2.6)$$

where the reaction function,

$$R(E) = \frac{\tan(k'a)}{k'a}. \quad (2.7)$$

Since the scattering function has unit magnitude we can also write it

$$S(E) = e^{i\theta(E)} = e^{-2ika} e^{i\theta'(E)}, \quad (2.8)$$

where $\theta(E)$ is the phase shift of the scattered wave relative to the case for which $V_0 = 0$. It is straightforward to show that

$$\tan(\theta') = \frac{2kaR(E)}{1 - k^2a^2R(E)^2} \quad \text{and} \quad \tan\left(\frac{\theta'}{2}\right) = kaR(E). \quad (2.9)$$

The time delay of the scattered particle due to its interaction with the barrier, V_0 , is given by

$$\tau \equiv \hbar \frac{d\theta}{dE} \Big|_{k=k_0}. \quad (2.10)$$

This time delay is called the *Wigner delay time* [[18]].

For the scattering system we consider here, the phase angle, $\theta'(E)$ is given by

$$\theta'(E) = 2\arctan\left[\frac{\beta}{\beta'}\tan(\beta'a)\right], \quad (2.11)$$

where $\beta = ka$ and $\beta' = k'a$. The Wigner delay time is given by

$$\begin{aligned} \tau(E) &= \hbar \frac{d\theta(E)}{dE} \\ &= \frac{2ma^2}{\hbar^2} \left(\frac{1}{\beta'^2 + \beta^2 \tan(\beta')^2} \left[\left(\frac{\beta'}{\beta} - \frac{\beta}{\beta'} \right) \tan(\beta') + \beta \sec(\beta')^2 \right] \right) - \frac{2ma^2}{\hbar\beta}. \end{aligned} \quad (2.12)$$

In Fig. (2.a) we show the phase angle, $\theta(E)$, as a function of energy, and in Fig. (2.b), we show the Wigner delay time for parameter values, $\hbar = 1$, $m = 1$, $a = 1$, and $V_0 = 10$. The peaks in Fig. (2.b) occur at values of the energy where the particle wave resonates with the barrier region. The fact that the Wigner delay time goes negative for low energies means that when $V_0 \neq 0$, the particle can be reflected earlier by the barrier, V_0 , than it would be if $V_0 = 0$.

In Fig. (3), we show that exact energy eigenstates as a function of position for a range of energies. At resonant energies, the energy eigenfunctions have enhanced probability in the scattering region. These resonances are also often called *quasibound states* because they are associated with complex energy poles of the scattering function. In Fig. (4), we plot those complex energy poles of $S(E)$ which give rise to the first three resonance peaks in the Wigner delay time. It is important to note that for scattering systems with higher space dimension, complex energy poles can have a profound effect on the scattering properties. For example, in two dimensional electron wave guides they can completely block transmission in some channels [[15]], [[16]].

3 Scattering Hamiltonian

Most of the interesting information regarding scattering events is contained in the energy dependence of the scattering phase shifts and in the location of

quasibound state poles. However, we generally cannot find those quantities exactly as we did in the previous section. There are a number of techniques for finding them if the scattering potential is weak, but not if the scattering potential is strong. In subsequent sections, we describe an approach to scattering theory which can deal with strong interactions, provided they are confined to a localized region of space. As we mentioned in Sect. (1), this approach to scattering theory was originally developed to deal with nuclear scattering processes, but recently has provided an important tool for studying universal properties of scattering processes induced by underlying chaos. We shall use this alternate approach to scattering theory to study the system considered in Sect. (2), and a similar system with a random scattering potential. In this way, we can compare its predictions to the exact results which were obtained in Sect. (2).

Let \hat{x} denote the position operator and let $|x\rangle$ denote its eigenstates, so that $\hat{x}|x\rangle = x|x\rangle$. The position eigenstates satisfy a completeness relation, $\int_{-\infty}^{\infty} dx |x\rangle\langle x| = \hat{1}$, where $\hat{1}$ is the unit operator, and they are delta normalized, $\int_{-\infty}^{\infty} dx \langle x|x' \rangle = \delta(x - x')$. Since the potential energy is infinite for $x < 0$, all states will be zero in that region. We can divide the completeness relation into three parts, $\hat{N} = \int_{-\infty}^0 dx |x\rangle\langle x|$, $\hat{Q} = \int_0^a dx |x\rangle\langle x|$, and $\hat{P} = \int_a^{\infty} dx |x\rangle\langle x|$, so that $\hat{N} + \hat{Q} + \hat{P} = \hat{1}$. However, the operator \hat{N} acting on any state gives zero because the potential energy is infinite in that region. Therefore, we can remove \hat{N} from the completeness relation without changing our final results. Thus, from now on we will write the completeness relation as $\hat{Q} + \hat{P} = \hat{1}$.

The operators, \hat{Q} and \hat{P} , are projection operators. They have the property that $\hat{Q} = \hat{Q}^2$, $\hat{P} = \hat{P}^2$, and $\hat{Q}\hat{P} = \hat{P}\hat{Q} = 0$. This is easily checked by explicit calculation. The operator \hat{Q} projects any state or operator onto the interval, $0 \leq x \leq a$, while the operator \hat{P} projects any state or operator onto the interval, $a \leq x \leq \infty$. In other words, if the state, $|\Psi\rangle$ has spatial dependence, $\Psi(x) \equiv \langle x|\Psi\rangle$, over the interval $(0 < x < \infty)$, then the state $\langle x|\hat{Q}|\Psi\rangle = \Psi(x)$ for $(0 < x < a)$ and the state $\langle x|\hat{P}|\Psi\rangle = \Psi(x)$ for $(a < x < \infty)$.

Inside the Region I, ($0 < x < a$) in Fig.(1), we define a Hamiltonian,

$$\hat{H}_{QQ} \equiv \hat{Q} \left(\frac{1}{2m} \hat{p}^2 + V_0 \right) \hat{Q}, \quad (3.1)$$

where \hat{p} is the momentum operator and m is the mass of the particle. The Hamiltonian, \hat{H}_{QQ} , is Hermitian and therefore it will have a complete, orthonormal set of eigenstates which we denote as $\hat{Q}|\phi_j\rangle$. We can write the eigenvalue problem in the region, $0 < x < a$, as $\hat{H}_{QQ}\hat{Q}|\phi_j\rangle = \lambda_j \hat{Q}|\phi_j\rangle$, where λ_j is the j^{th} energy eigenvalue of \hat{H}_{QQ} and $j = 1, 2, \dots \infty$. Because there is an infinitely hard wall at $x = 0$, the eigenstates $\phi_j(x) \equiv \langle x|\hat{Q}|\phi_j\rangle$ must be zero at $x = 0$. We have some freedom in choosing the boundary condition at $x = a$ and we will do that later. The completeness of the states, $\hat{Q}|\phi_j\rangle$, allows us to write the completeness relation, $\sum_j \hat{Q}|\phi_j\rangle\langle\phi_j|\hat{Q} = \hat{Q}$. Orthonormality requires that $\langle\phi_j|\hat{Q}|\phi_{j'}\rangle = \delta_{j,j'}$.

The Hamiltonian for the region, $a < x < \infty$, can be written

$$\hat{H}_{PP} \equiv \hat{P} \left(\frac{1}{2m} \hat{p}^2 \right) \hat{P}. \quad (3.2)$$

Its eigenvalues are continuous and have range, ($0 \leq E \leq \infty$). The eigenvector of \hat{H}_{PP} , with eigenvalue, E , will be denoted $\hat{P}|E\rangle$. The eigenvalue equation then reads, $\hat{H}_{PP}\hat{P}|E\rangle = E\hat{P}|E\rangle$.

Any state, $|\Psi\rangle$, can be decomposed into its contributions from the two disjoint regions of configuration space as $|\Psi\rangle = \hat{Q}|\Psi\rangle + \hat{P}|\Psi\rangle$. We can expand $\hat{Q}|\Psi\rangle$ in terms of the complete set of states, $\hat{Q}|\phi_j\rangle$ and we obtain,

$$|\Psi\rangle = \sum_j \beta_j \hat{Q}|\phi_j\rangle + \hat{P}|\Psi\rangle, \quad (3.3)$$

where $\beta_j = \langle\phi_j|\hat{Q}|\Psi\rangle$. The function $\langle x|\hat{Q}|\Psi\rangle$ must be equal to the function, $\langle x|\hat{P}|\Psi\rangle$, at the interface, $x = a$. In addition, the slopes of these two functions must be equal at the interface.

We couple the two regions of configuration space, at their interface, with the singular operator, $\hat{V} = C\delta(\hat{x} - a)\hat{p}$. The coupling constant, C , will be determined later. Then

$$\hat{H}_{QP} = \hat{Q}\hat{V}\hat{P} = C \int_0^a dx_1 \int_a^\infty dx_0 |x_1\rangle \delta(x_1 - x_0) \delta(x_0 - a) \frac{d}{dx_0} \langle x_0|, \quad (3.4)$$

and

$$\hat{H}_{PQ} = \hat{P}\hat{V}\hat{Q} = C \int_a^\infty dx_0 \int_0^a dx_1 |x_0\rangle \delta(x_0 - x_1) \delta(x_1 - a) \frac{d}{dx_1} \langle x_1|. \quad (3.5)$$

It is useful to remember that $\int_0^a dx \delta(x - a) = \frac{1}{2}$, $\int_0^a dx \delta(x - x_0) = 1$ if $0 < x_0 < a$, and $\int_0^a dx \delta(x - x_0) = 0$ if $a < x_0$. Note also that

$$\hat{H}_{QQ} = \int_0^a dx |x\rangle \left(\frac{-\hbar^2}{2m} \frac{d^2}{dx^2} + V_0 \right) \langle x| \quad (3.6)$$

and

$$\hat{H}_{PP} = \int_a^\infty dx |x\rangle \left(\frac{-\hbar^2}{2m} \frac{d^2}{dx^2} \right) \langle x| \quad (3.7)$$

The total Hamiltonian of the system can be written

$$\hat{H} = \hat{H}_{QQ} + \hat{H}_{PP} + \hat{H}_{QP} + \hat{H}_{PQ}. \quad (3.8)$$

The energy eigenstates, $|E\rangle$, satisfy the eigenvalue equation $\hat{H}|E\rangle = E|E\rangle$. The energy eigenstates can be decomposed into their contributions from the two regions of configuration space, so that

$$|E\rangle = \sum_j \gamma_j \hat{Q}|\phi_j\rangle + \hat{P}|E\rangle, \quad (3.9)$$

where $\gamma_j = \langle \phi_j | \hat{Q} | E \rangle$. The eigenvalue equation then takes the form

$$\begin{pmatrix} \hat{H}_{QQ} & 0 & \dots & \hat{H}_{QP} \\ 0 & \hat{H}_{QQ} & \dots & \hat{H}_{QP} \\ \vdots & \vdots & \ddots & \vdots \\ \hat{H}_{PQ} & \hat{H}_{PQ} & \dots & \hat{H}_{PP} \end{pmatrix} \begin{pmatrix} \gamma_1 \hat{Q}|\phi_1\rangle \\ \gamma_2 \hat{Q}|\phi_2\rangle \\ \vdots \\ \hat{P}|E\rangle \end{pmatrix} = E \begin{pmatrix} \gamma_1 \hat{Q}|\phi_1\rangle \\ \gamma_2 \hat{Q}|\phi_2\rangle \\ \vdots \\ \hat{P}|E\rangle \end{pmatrix} \quad (3.10)$$

This yields a series of equations

$$\hat{H}_{QQ}|\phi_j\rangle \gamma_j + \hat{H}_{QP}|E\rangle = E\hat{Q}|\phi_j\rangle \gamma_j, \quad (3.11)$$

for $j = 1, 2, \dots$ and

$$\hat{H}_{PP}|E\rangle + \sum_j H_{PQ}|\phi_j\rangle \gamma_j = E\hat{P}|E\rangle. \quad (3.12)$$

Before we can proceed further, we must find conditions for Hermiticity of the Hamiltonian, \hat{H} .

4 Hermiticity Condition

Consider the arbitrary states, $|\Psi\rangle$ and $|\Xi\rangle$. The condition for Hermiticity of these states is that

$$\langle \Xi | \hat{H} | \Psi \rangle - \langle \Psi | \hat{H} | \Xi \rangle^* = 0. \quad (4.1)$$

We can decompose the states $|\Psi\rangle$ and $|\Xi\rangle$ into their contributions to the two disjoint configuration space regions and write them in the form,

$$|\Psi\rangle = \hat{Q}|\Psi\rangle + \hat{P}|\Psi\rangle = \sum_j \beta_j \hat{Q}|\phi_j\rangle + \hat{P}|\Psi\rangle, \quad (4.2)$$

where $\beta_j = \langle \phi_j | \hat{Q} | \Psi \rangle$ and

$$|\Xi\rangle = \hat{Q}|\Xi\rangle + \hat{P}|\Xi\rangle = \sum_j \alpha_j \hat{Q}|\phi_j\rangle + \hat{P}|\Xi\rangle, \quad (4.3)$$

where $\alpha_j = \langle \phi_j | \hat{Q} | \Xi \rangle$. In the interior region, we have expanded $|\Psi\rangle$ and $|\Xi\rangle$ in terms of the complete set of energy eigenstates, $\hat{Q}|\phi_j\rangle$, of the Hamiltonian, \hat{H}_{QQ} . To simplify the notation, let $|\psi_j\rangle \equiv \beta_j \hat{Q}|\phi_j\rangle$, $|\xi_j\rangle \equiv \alpha_j \hat{Q}|\phi_j\rangle$, $\hat{P}|\Psi\rangle = |\Psi_P\rangle$, and $\hat{P}|\Xi\rangle = |\Xi_P\rangle$. The states can be written

$$|\Xi\rangle = \begin{pmatrix} |\xi_1\rangle \\ |\xi_2\rangle \\ \vdots \\ |\Xi_P\rangle \end{pmatrix} \quad \text{and} \quad |\Psi\rangle = \begin{pmatrix} |\psi_1\rangle \\ |\psi_2\rangle \\ \vdots \\ |\Psi_P\rangle \end{pmatrix}. \quad (4.4)$$

If we note that

$$\begin{aligned} \langle \Xi | \hat{H} | \Psi \rangle &= (\langle \xi_1 |, \langle \xi_2 |, \dots, \langle \Xi_P |) \begin{pmatrix} \hat{H}_{QQ} & 0 & \dots & \hat{H}_{QP} \\ 0 & \hat{H}_{QQ} & \dots & \hat{H}_{QP} \\ \vdots & \vdots & \ddots & \vdots \\ \hat{H}_{PQ} & \hat{H}_{PQ} & \dots & \hat{H}_{PP} \end{pmatrix} \begin{pmatrix} |\psi_1\rangle \\ |\psi_2\rangle \\ \vdots \\ |\Psi_P\rangle \end{pmatrix} \\ &= \sum_j \langle \xi_j | \hat{H}_{QQ} | \psi_j \rangle + \sum_j \langle \xi_j | \hat{H}_{QP} | \Psi_P \rangle + \sum_j \langle \Xi_P | \hat{H}_{PQ} | \psi_j \rangle + \langle \Xi_P | \hat{H}_{PP} | \Psi_P \rangle, \end{aligned} \quad (4.5)$$

then the condition for Hermiticity is

$$\langle \Xi | \hat{H} | \Psi \rangle - \langle \Psi | \hat{H} | \Xi \rangle^* = \sum_j [\langle \xi_j | \hat{H}_{QQ} | \psi_j \rangle - \langle \psi_j | \hat{H}_{QQ} | \xi_j \rangle^*]$$

$$\begin{aligned}
& + \sum_j [\langle \xi_j | \hat{H}_{QP} | \Psi_P \rangle - \langle \psi_j | \hat{H}_{QP} | \Xi_P \rangle^*] + \sum_j [\langle \Xi_P | \hat{H}_{PQ} | \psi_j \rangle - \langle \Psi_P | \hat{H}_{PQ} | \xi_j \rangle^*] \\
& + [\langle \Xi_P | \hat{H}_{PP} | \Psi_P \rangle - \langle \Psi_P | \hat{H}_{PP} | \Xi_P \rangle^*] = 0. \tag{4.6}
\end{aligned}$$

We can now evaluate Eq. (4.6) term by term. Let $\langle x | \psi_j \rangle \equiv \psi_j(x)$, $\langle x | \xi_j \rangle \equiv \xi_j(x)$, $\langle x | \Xi_P \rangle \equiv \Xi_P(x)$ and $\langle x | \Psi_P \rangle \equiv \Psi_P(x)$. Then

$$\begin{aligned}
\langle \Xi | \hat{H} | \Psi \rangle - \langle \Psi | \hat{H} | \Xi \rangle^* & = -\frac{\hbar^2}{2m} \sum_j \left(\xi_j^*(a) \frac{d\psi_j}{dx} \Big|_a - \psi_j^*(a) \frac{d\xi_j}{dx} \Big|_a \right) \\
& + \frac{C}{4} \sum_j \left(\xi_j^*(a) \frac{d\Psi_P}{dx} \Big|_a - \psi_j^*(a) \frac{d\Xi_P}{dx} \Big|_a \right) + \frac{C}{4} \sum_j \left(\Xi_P^*(a) \frac{d\psi_j}{dx} \Big|_a - \Psi_P^*(a) \frac{d\xi_j}{dx} \Big|_a \right) \\
& - \frac{\hbar^2}{2m} \left(\Xi_P^*(a) \frac{d\Psi_P}{dx} \Big|_a - \Psi_P^*(a) \frac{d\Xi_P}{dx} \Big|_a \right) = 0, \tag{4.7}
\end{aligned}$$

is the Hermiticity condition. For our subsequent discussion, it is useful to note that for the special case when the eigenstate, $\phi_j(x)$, has zero slope on the interface, so $\frac{d\phi_j}{dx} \Big|_a = 0$, the Hermiticity condition reduces to

$$\begin{aligned}
\langle \Xi | \hat{H} | \Psi \rangle - \langle \Psi | \hat{H} | \Xi \rangle^* & = \frac{C}{4} \sum_j \left(\xi_j^*(a) \frac{d\Psi_P}{dx} \Big|_a - \psi_j^*(a) \frac{d\Xi_P}{dx} \Big|_a \right) \\
& - \frac{\hbar^2}{2m} \left(\Xi_P^*(a) \frac{d\Psi_P}{dx} \Big|_a - \Psi_P^*(a) \frac{d\Xi_P}{dx} \Big|_a \right) = 0, \tag{4.8}
\end{aligned}$$

If we let $|\Psi\rangle = |E\rangle$ and $|\Xi\rangle = |E\rangle$ in Eq. (4.8), the Hermiticity condition reduces to

$$\frac{C}{4} \sum_j \gamma_j \phi_j(a) = \frac{\hbar^2}{2m} \Psi_{E,P}(a), \tag{4.9}$$

where $\Psi_{E,P}(x) = \langle | \hat{P} | E \rangle$. This Hermiticity condition allows us to determine the coupling constant, C . If we remember that $\langle x | \hat{Q} | E \rangle = \sum_j \gamma_j \phi_j(x)$, then continuity of the energy eigenfunction at $x = a$ requires that

$$C = \frac{2\hbar^2}{m}. \tag{4.10}$$

Thus, the Hermiticity condition allows us to determine the strength of the coupling at the interface.

5 The Reaction Function

We can use the formalism derived in Sections (3) and (4) to derive an expression for the reaction function, $R(E)$. Let us return to Eq. (3.11). If we multiply by $\langle \phi_j | \hat{Q}$, use Eq. (3.4), and the normalization condition, $\langle \phi_j | \hat{Q} | \phi_j \rangle = 1$, we obtain

$$(\lambda_j - E)\gamma_j + \frac{C}{4}\phi_j^*(a) \frac{d\Psi_R^0}{dx} \Big|_a = 0. \quad (5.1)$$

Similarly, if we multiply Eq. (3.12) by $\langle E | \hat{P}$, we obtain

$$\begin{aligned} & -\frac{\hbar^2}{2m} \int_a^\infty dx \Psi_{E,P}^*(x) \frac{d^2\Psi_{E,P}}{dx^2} + \frac{C}{4} \sum_j \Psi_{E,P}^*(a) \frac{d\phi_j}{dx} \Big|_a \gamma_j \\ & = E \int_a^\infty dx \Psi_{E,P}^*(x) \Psi_{E,P}(x), \end{aligned} \quad (5.2)$$

where $\Psi_{E,P}(x) \equiv \langle x | \hat{P} | E \rangle$.

Before we can proceed further, we must decide on boundary conditions for our states, $\phi_j(x)$. We can use any complete basis set in the region, $0 < x < a$, provided they have the property $\phi_j(0) = 0$. We are free to choose the boundary condition at $x = a$. We have seen in Eq. (4.8) that the Hermiticity condition becomes especially simple for the boundary condition, $\frac{d\phi_j(x)}{dx} \Big|_a = 0$. Therefore, that is the boundary condition that we will use here. The states with these boundary conditions are given by $\phi_j(x) = \sqrt{\frac{2}{a}} \sin\left(\frac{j\pi x}{2a}\right)$, for j odd ($j = 1, 3, \dots$), and the corresponding eigenvalues are $\lambda_j = \frac{\hbar^2\pi^2 j^2}{8a^2 m} + V_0$. The states, $\phi_j(x)$ and the eigenvalues, λ_j , should not be confused with the exact energy eigenvalues and eigenstates in Region I. The states, $\phi_j(x)$, only serve to provide us a complete set of states in Region I which can then be used to construct the exact energy eigenstates in Region I. With these boundary conditions, Eq. (5.2) takes the form

$$-\frac{\hbar^2}{2m} \int_a^\infty dx \Psi_{E,P}^*(x) \frac{d^2\Psi_{E,P}}{dx^2} = E \int_a^\infty dx \Psi_{E,P}^*(x) \Psi_{E,P}(x). \quad (5.3)$$

Let us now show that this description of the system leads to well known results. We can derive the reaction function originally obtained by Wigner and

Eisenbud. Let us return to Eq. (5.1) and solve for γ_j . We find

$$\gamma_j = \frac{\hbar^2}{2m} \frac{1}{E - \lambda_j} \phi_j^*(a) \frac{d\Psi_{E,P}}{dx} \Big|_a. \quad (5.4)$$

If we combine Eqs. (4.9) and (5.4), we obtain

$$\Psi_{E,P}(a) = \frac{\hbar^2}{2m} \sum_j \frac{\phi_j^*(a) \phi_j(a)}{E - \lambda_j} \frac{d\Psi_{E,P}}{dx} \Big|_a. \quad (5.5)$$

From Eq. (5.5), we can express the logarithmic derivative of the outside wavefunction, $\frac{d\Psi_E^0}{dx} \frac{a}{\Psi_{E,P}}$, evaluated at the interface (and therefore the reaction function, $R(E)$), in terms of the inside states. We find

$$R(E) \equiv \frac{\Psi_{E,P}(a)}{a \frac{d\Psi_{E,P}}{dx} \Big|_a} = \frac{\hbar^2}{2ma} \sum_j \frac{\phi_j^*(a) \phi_j(a)}{E - \lambda_j}. \quad (5.6)$$

For scattering in higher dimensional space or for systems with internal degrees of freedom the reaction function becomes a matrix and is then called the *reaction matrix*.

In Eq. (2.8), we obtained an exact expression for the reaction function. If we equate Eqs. (2.8) and (5.6), we obtain

$$R(E) = \frac{\tan(k'a)}{k'a} = \frac{\hbar^2}{2ma} \sum_j \frac{\phi_j^*(a) \phi_j(a)}{E - \lambda_j} = \frac{\hbar^2}{ma^2} \sum_{j=1}^{\infty} \frac{\sin^2\left(\frac{(2j-1)\pi}{2}\right)}{E - \frac{\hbar^2\pi^2(2j-1)^2}{8a^2m} - V_0}, \quad (5.7)$$

for j odd. Let $\kappa^2 = \frac{2mV_0}{\hbar^2}$. Then we can write Eq. (5.7) in the form

$$\frac{\tan(\sqrt{k^2 - \kappa^2}a)}{\sqrt{k^2 - \kappa^2}a} = \frac{2}{a^2} \sum_{\substack{j=1 \\ odd}}^{\infty} \frac{1}{k^2 - \kappa^2 - \frac{\pi^2(2j-1)^2}{4a^2}} \quad (5.8)$$

From Ref. [[17]] one can show that this is just the definition of the series expansion of the tangent function in terms of its argument.

The reaction function can also be expressed as a product of matrices. Let us consider the first N eigenvalues and eigenvectors of the the Hamiltonian, \hat{H}_{QQ} (we later let $N \rightarrow \infty$). We then write the Hamiltonian, \hat{H}_{QQ} , in the matrix

representation in which it is diagonal (in this representation we denote it as \bar{H}_{in}^N), and obtain

$$\bar{H}_{in}^N = \begin{pmatrix} \lambda_1 & 0 & \dots & 0 \\ 0 & \lambda_2 & \dots & 0 \\ \vdots & \vdots & \ddots & \vdots \\ 0 & 0 & \dots & \lambda_N \end{pmatrix}. \quad (5.9)$$

We also introduce the vector of eigenstates of \hat{H}_{QQ} , but evaluated at the interface,

$$\bar{v}_N = \sqrt{\frac{\hbar^2}{2ma}} \begin{pmatrix} \phi_1(a) \\ \phi_2(a) \\ \vdots \\ \phi_N(a) \end{pmatrix}. \quad (5.10)$$

Then the reaction function can be written in the compact form

$$R_N(E) = \bar{v}_N^\dagger \frac{1}{E\bar{1}_N - \bar{H}_{in}^N} \bar{v}_N = \frac{\hbar^2}{2ma} \sum_j^N \frac{\phi_j^*(a)\phi_j(a)}{E - \lambda_j}, \quad (5.11)$$

where $\bar{1}_N$ is the $N \times N$ dimensional unit matrix and \bar{v}_N^\dagger denotes the Hermitian adjoint of \bar{v}_N .

6 The Scattering Function

It is useful to express the scattering function, $S(E)$, in matrix notation, because we can then find a very interesting expression for the complex energy poles of $S(E)$. In Eq. (2.7), we obtained an expression for the scattering function in terms of the reaction function. In terms of the truncated reaction function it is

$$S_N(E) = e^{-2ika} \left[\frac{1 + ikaR_N(E)}{1 - ikaR_N(E)} \right], \quad (6.1)$$

where

$$R_N(E) = \frac{\hbar^2}{ma^2} \sum_{j=1}^N \frac{\sin^2\left(\frac{(2j-1)\pi}{2}\right)}{E - \frac{\hbar^2\pi^2(2j-1)^2}{8a^2m} - V_0}. \quad (6.2)$$

In Table (1), we give the positions of the three lowest energy quasibound state poles found by using the exact expression for $R(E)$ given in Eq. (2.8). These values are exact to the number of digits shown. Also in Table (1), we give the

Table 1: comparison of pole positions with exact result

n	First Pole	Second Pole	Third Pole
250	17.9812 -5.0071	45.0729 -17.6046	93.2048 -34.5167
350	17.9771 -4.9999	45.0197 -17.5295	92.8700 -34.2099
500	17.9742 -4.9945	44.9806 -17.4736	92.6336 -33.9798
1000	17.9707 -4.9883	44.9359 -17.4089	92.3725 -33.7124
exact	17.9672 -4.9821	44.8921 -17.3448	92.1262 -33.4466

positions of those poles found by using Eq. (6.1) for four different truncations, $N = 250$, $N = 350$, $N = 500$, and $N = 1000$. The values obtained using Eq. (6.1) converge slowly to the correct answer.

The scattering function can be written in several other forms as well. Let us introduce the column vector,

$$\bar{w}_N = \sqrt{ka} \bar{v}_N = \sqrt{\frac{\hbar^2 k}{2m}} \begin{pmatrix} \phi_1(a) \\ \phi_2(a) \\ \vdots \\ \phi_N(a) \end{pmatrix}. \quad (6.3)$$

Then the scattering function becomes

$$S_N(E) = e^{-2ika} \left[\frac{1 + iK_N}{1 - iK_N} \right] = e^{-2ika} \left[1 + \frac{2iK_N}{1 - iK_N} \right]. \quad (6.4)$$

where

$$K_N \equiv \bar{w}_N^\dagger \frac{1}{E\bar{1}_N - \bar{H}_{in}^N} \bar{w}_N. \quad (6.5)$$

Using Eq. (6.4), we can write (we suppress the index N)

$$\begin{aligned} \frac{K}{1 - iK} &= \frac{1}{1 - i\bar{w}^\dagger \frac{1}{E\bar{1} - \bar{H}_{in}} \bar{w}} \bar{w}^\dagger \frac{1}{E\bar{1} - \bar{H}_{in}} \bar{w} \\ &= \sum_{n=0}^{\infty} (i)^n \bar{w}^\dagger \left(\frac{1}{E\bar{1} - \bar{H}_{in}} \bar{w} \bar{w}^\dagger \right)^n \frac{1}{E\bar{1} - \bar{H}_{in}} \bar{w} \\ &= \bar{w}^\dagger (E\bar{1} - \bar{H}_{in}) \left(\frac{1}{E\bar{1} - \bar{H}_{in} - i\bar{w}\bar{w}^\dagger} \right) \frac{1}{E\bar{1} - \bar{H}_{in}} \bar{w}, \end{aligned} \quad (6.6)$$

The scattering function, $S_N(E)$, can now be written in the form

$$S_N(E) = 1 + 2i\bar{w}_N^\dagger (E\bar{1}_N - \bar{H}_{in}^N) \frac{\bar{M}}{\text{Det}[E\bar{1}_N - \bar{H}_{in}^N - i\bar{w}_N \bar{w}_N^\dagger]} \frac{1}{E\bar{1}_N - \bar{H}_{in}^N} \bar{w}_N. \quad (6.7)$$

where \bar{M} is the adjoint of the matrix, $E\bar{1} - \bar{H}_{in} - i\bar{w}\bar{w}^\dagger$, and Det denotes its determinant.

The poles of the scattering function are given by the condition

$$\text{Det}[E\bar{1}_N - \bar{H}_{in}^N - i\pi\bar{w}_N\bar{w}_N^\dagger] = 0. \quad (6.8)$$

Eq. (6.8) gives an N^{th} order polynomial in E whose solutions are the complex energies which locate the poles. At first sight, it would appear that the complex energy poles of the scattering function are simply given by the eigenvalues of the non-Hermitian matrix, $\bar{H}_{eff}^N \equiv \bar{H}_{in}^N + i\pi\bar{w}_N\bar{w}_N^\dagger$. However, the column matrices, \bar{w}_N depend on energy, E , and therefore the eigenvalues, $\mu_i(E)$, of \bar{H}_{eff}^N also depend on energy, E .

In Fig. (5), we locate the zeros of $\text{Det}[E\bar{1} - \bar{H}_{eff}] = \text{Det}[E\bar{1} - \bar{H}_{eff} - i\pi\bar{w}\bar{w}^\dagger]$ in the neighborhood of the first three resonance energies. The zeros satisfy the equation,

$$\text{Det}[E\bar{1} - \bar{H}_{eff}] = (E - \mu_1(E))(E - \mu_2(E)) \times \dots \times (E - \mu_N(E)). \quad (6.9)$$

In Fig. (5.a) we plot $(E - \mu_1(E))$ versus E for complex values of E in the neighborhood of the first pole. We see that $(E - \mu_1(E)) = 0$ at the energy of the first pole. In Figs. (5.b) and (5.c), we plot $(E - \mu_1(E))$ and $(E - \mu_2(E))$ at the energies of the second and third poles, respectively. Again we see that they go to zero at the energies of their respective poles.

7 Random potential

The potential used in Section (2), is a smooth step function which allows us to solve the scattering problem exactly. It also allows us to obtain exact expressions for the basis state energies, λ_j and coupling constants, \bar{v}_N . For our simple scattering problem, matrix elements of \bar{v}_N simply alternate between two constant values.

We now use these same methods to study scattering from a random step potential. The random potential we use is a sequence of 10 tent-like shapes

(upright or inverted) on the interval $0 < x < a$ with $a = 100$. We again choose $\hbar = 1$ and $m = 1$. We can express the potential in the form

$$V(x) = \begin{cases} 10 + \sum_{j=0}^9 v_j \frac{(x-10j)}{5} & \text{for } 10j < x < 10j + 5; \\ 10 + \sum_{j=0}^9 v_j \frac{(10j+10-x)}{5} & \text{for } 10j + 5 < x < 10j + 10; \\ 0 & \text{otherwise.} \end{cases} \quad (7.1)$$

The values of v_j are chosen to lie in the interval, $-0.5 \leq v_j \leq +0.5$ with uniform distribution over that interval. One hundred different realizations of this potential are shown in Fig. 6.

For this larger value of a , there are about 10 to 12 scattering resonance peaks in the energy interval $10.5 \leq E \leq 11$. To find the eigenvalues and eigenfunctions for this random potential we used an implicit finite difference method. When there is no randomness ($v_j = 0$ for all j), the Wigner delay time can be calculated exactly as we showed in Section 2. Fig. (7) shows the Wigner delay times when $v_j = 0$ for all j . In Figure (7), the exact result is given by the solid line and the approximate result obtained by using the reaction matrix series expansion, Eq. (5.6), is given by the discrete dots. The agreement is excellent. In Fig. (8), we plot the values of W_n which are obtained from the 100 hundred realizations of the random potential when $a = 100$. The peak points (positive and negative) on the oscillating solid line give values of W_n for the case $v_j = 0$ for all j . We see that the higher eigenmodes are not affected by the random potential.

In Fig. (9), we show the Wigner delay times for 100 different realizations of random potential. The positions of resonance peaks as well as their widths change with different potentials. In Fig. (10) we plot a histogram of values of the Wigner delay times shown in Figure (9). This is similar to distribution one can get from RMT calculations, except that our distribution has a longer tail (see [11] [19]). Finally, in Fig. (11) we show the distribution of Wigner delay time resonance widths. We find that the distribution of delay time widths is fairly symmetrically distributed around its average value.

As we can see, this approach allows us to compute the scattering properties

of a variety of shapes of scattering potential with great accuracy. The only constraint is that the scattering potential must occupy a well defined region of space.

8 Conclusions

The configuration space scattering picture, described in Sections (3)-(6) is a basis for Weidenmuller's phenomenological Hamiltonian theory of nuclear scattering, and it has provided a framework to look for universal behavior in the scattering properties of open quantum systems whose underlying classical counterparts are chaotic. There is now a large body of work [7] which shows that bounded quantum systems, whose underlying classical dynamics is chaotic, have energy eigenvalues and energy eigenfunction which have statistical properties similar to those of certain types of random Hamiltonian matrices. Similar questions are being asked about the scattering properties of open quantum systems. For open systems, one can look at the statistical properties of the spacings and widths of scattering resonances, and of Wigner delay times.

The theory described in Sections (3)-(6) can be used to compare the results of laboratory and numerical experiments to random Hamiltonian matrix predictions. For example, for scattering systems in which no magnetic fields are present, the Hamiltonian, H_{in} , which is formed from the eigenvalues of H_{QQ} , is replaced by a Hamiltonian, H_{in}^{rm} , which is formed from the eigenvalues of a Hamiltonian matrix whose matrix elements are random numbers which are Gaussian distributed. The elements of the coupling matrix, \bar{w} , are also chosen from a random distribution. The strength of the coupling constant, C , is left as a variable parameter in these random matrix theories. The random matrix theory predictions are in qualitative agreement with numerical experiments and some laboratory experiments.

However, a number of assumptions underly the random matrix theory predictions, and there are a number of issues that remain open. For actual scattering systems, the coupling constant, C , is fixed by the detailed dynamics using the Hermiticity condition, but in random matrix theories it is a variable parameter. In random matrix theories, the coupling matrix, \bar{w} , is chosen from a random distribution. How does it actually look for a deterministic system with underlying

classical chaos? This has never been studied.

Random matrix theories also neglect the dependence of H_{eff} on the energy, E . The actual error made in making this assumption needs to be understood. For two dimensional electron waveguides, there is an additional problem that at the threshold energy where a new channel opens, quasibound states inside the cavity can extend far down the leads. It is not clear how well the theory presented in Sections (3)-(6) and therefore the random matrix theory, can describe scattering in those regions. Never-the-less, this approach to scattering theory has allowed contact to be made between chaos theory and scattering theory for open quantum systems. As we have just shown, it can also provide a powerful tool to study scattering processes in atomic and mesoscopic devices, when intrinsic disorder in the medium needs to be included.

9 Acknowledgements

The authors wish to thank the Robert A. Welch Foundation Grant No. F-1051, NSF Grant No. INT-9602971, and DOE Contract No. DE-FG03-94ER14405 for partial support of this work. We thank NPACI and the University of Texas at Austin High Performance Computing Center for use of their computer facilities. We also thank German Luna Acosta and Gengis Sen ??????for helpful discussions.

References

- [1] P.L. Kapur and R. Peierls, “The dispersion formula for nuclear reactions”, Proc. Roy. Soc. (London) **A166** 277-295 (1938).
- [2] E.P. Wigner and L.E. Eisenbud, Phys. Rev. “Higher angular momenta and long range interaction in resonance reactions” **72** 29-41 (1949).
- [3] A.M. Lane and R.G. Thomas, “R-Matrix theory of Nuclear reactions” Rev. Mod. Phys. **30** 257-353 (1958).
- [4] C. Bloch, “Une formulation unifiée de la théorie des réactions nucléaires”, Nuclear Physics **4** 503-512 (1957).
- [5] H. Feshbach, “A unified theory of nuclear reactions. II”, Ann. Phys. **19** 287-313 (1962).
- [6] C. Mahaux and H.A. Weidenmuller, *Shell-Model Approach to Nuclear Reactions* (North-Holland Pub. Co., Amsterdam, 1969).
- [7] L.E. Reichl, *The transition to Chaos in Conservative Classical Systems: Quantum Manifestations* (Spring-Verlag, New York, 1992).
- [8] T. Guhr, A. Muller-Groeling, and H.A. Weidenmuller, “Random-matrix theories in quantum physics:common concepts.” Phys. Rept. **299** 189-425 (1998).
- [9] A.G. Huibers, S.R. Patel, C.M. Marcus, P.W. Brouwer, C.I. Duruoz, and J.S. Harris, Jr., “Distributions of the conductance and its parametric derivatives in quantum dots” Phys. Rev. Lett. **81** 1917-20 (1998).
- [10] C. Ellegaard, T. Guhr, K. Lindemann, H.Q. Lorensen, J. Nygard, and M. Oxborrow, “Spectral statistics of acoustic resonances in aluminum blocks.”, Phys. Rev. Lett. **75** 1546-51 (1995).

- [11] Akguc and Reichl, "Conductance and Statistical Properties of Chaotic and Integrable Electron Waveguides", *J. Stat. Phys.* **98** 813-34 (2000)
- [12] B.S. Pavlov, *Theor. Math. Phys.* **59** 544 (1984); "The theory of extensions and explicitly-soluble methods", *Russ. Math. Surveys* **42** 127-168 (1987).
- [13] Y.V. Fyodorov and H-J Sommers, "Statistics of resonance poles, phase shifts and time delays in quantum chaotic scattering: Random matrix approach for system with broken time-reversal invariance" *J.Math.Phys.bf* **38** 1918-1981 (1997).
- [14] S. Albeverio, F. Haake, P. Kurasov, M. Kus, P. Seba, "S-Matrix, resonances, and wave functions for transport through billiards with leads", *J. Math. Phys.* **37** 4888-4903 (1996).
- [15] Kyungsun Na and L.E. Reichl, "Electron conductance and lifetimes in a ballistic electron waveguide", *J. Stat. Phys.* **92** 519-542 (1998); Kyungsun Na and L.E. Reichl, "Effect of the quasibound states on quantum transport in a ballistic electron waveguide", *Phys. Rev. B* **59** 13073-9 (1999).
- [16] Suhan Ree and L.E. Reichl, "Aharonov-Bohm effect and resonances in the circular quantum billiard with two leads" *Phys. Rev. B* **59** 8163-9 (1999).
- [17] I.S. Gradshteyn and I.M. Ryzhik, *Table of Integrals, Series, and Products*, (Academic press, New York, 1980), no.1.421.
- [18] D. Bohm, *Quantum Theory* (Prentice-Hall, Inc. Englewood Cliffs, N.J., 1950), p. 260; E.P. Wigner, *Phys. Rev.* **98** 145 (1955); F.T. Smith, *Phys. Rev.* **118** 349 (1960).
- [19] Petr Seba, Karol Zyckowski and Jakub Zakrzewski, "Statistical properties of random scattering matrices", *Phys. Rev. E* **54** 2438-45 (1997)

Figure 1: The scattering potential, $V(x)$ for $\hbar = 1$, $V_0 = 10$, and $a = 1$.

Figure 2: (a) Phase θ of $S = \exp(i\theta)$ function, (b) Wigner delay time τ Both plot is as a function of energy for $\hbar = 1$, $V_0 = 10$, and $a = 1$. Three resonances are shown with arrows at the resonance energy values.

Figure 3: Absolute value of exact energy eigenstates plotted as a function of spatial variable, x , and energy, E , for $\hbar = 1$, $V_0 = 10$, and $a = 1$.

Figure 4: Poles of S function in the lower complex plane for $\hbar = 1$, $V_0 = 10$, and $a = 1$. The absolute value of S is plotted in logarithmic scale, as a function to real and imaginary parts of the energy.

Figure 5: (a) $E - \mu_1(E)$ versus $E = E_r + iE_i$ in the neighborhood of the first pole; (b) $E - \mu_2(E)$ versus $E = E_r + iE_i$ in the neighborhood of the second pole; (c) $E - \mu_3(E)$ versus $E = E_r + iE_i$ in the neighborhood of the third pole. All plots are for $\hbar = 1$, $V_0 = 10$, and $a = 1$.

Figure 6: One hundred realizations of the random potential, Eq. (7.1).

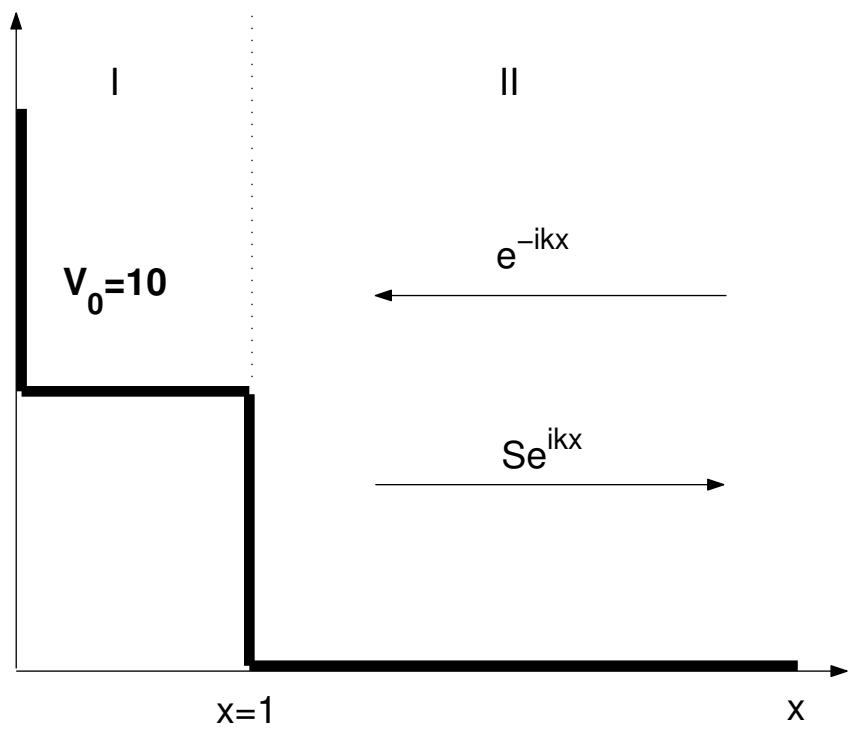
Figure 7: Wigner delay time for the step potential, $V(x) = 10$ for $0 < x < 100$ and $V(x) = 0$ for $x > 100$. The solid line is the exact result. The dots are obtained using the series approximation to the reactions matrix, Eq. (5.6)

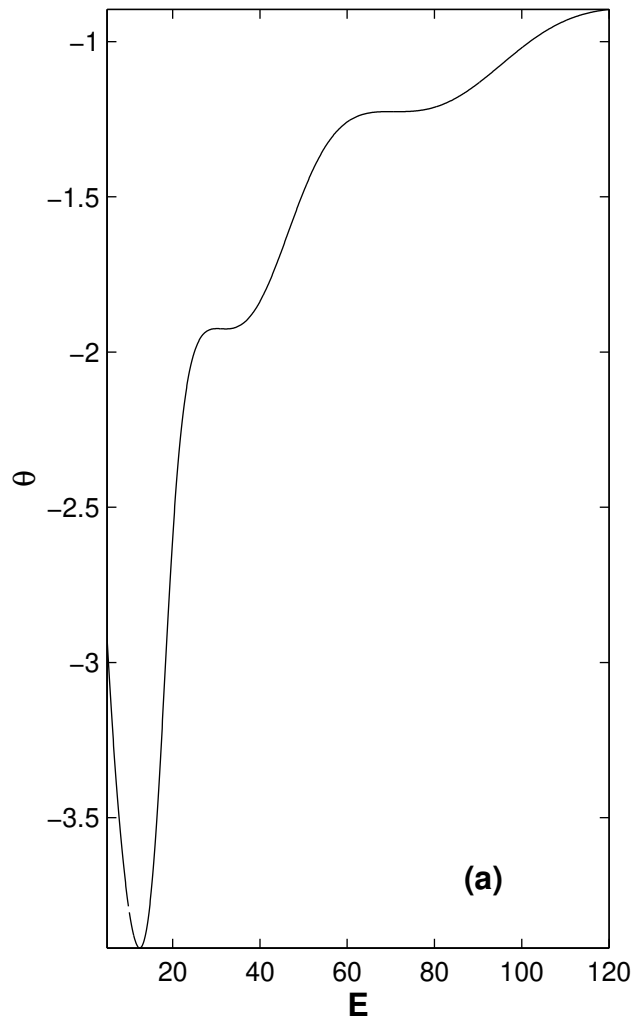
Figure 8: The coupling constants, W_n , for the 100 different realizations of random potential shown in Fig. (6). The peak values (positive and negative) of the solid line give the values of W_n for $v_j = 0$ and $V(x) = 10$.

Figure 9: Wigner delay times for the 100 realizations of the random potential shown in Fig. 6.

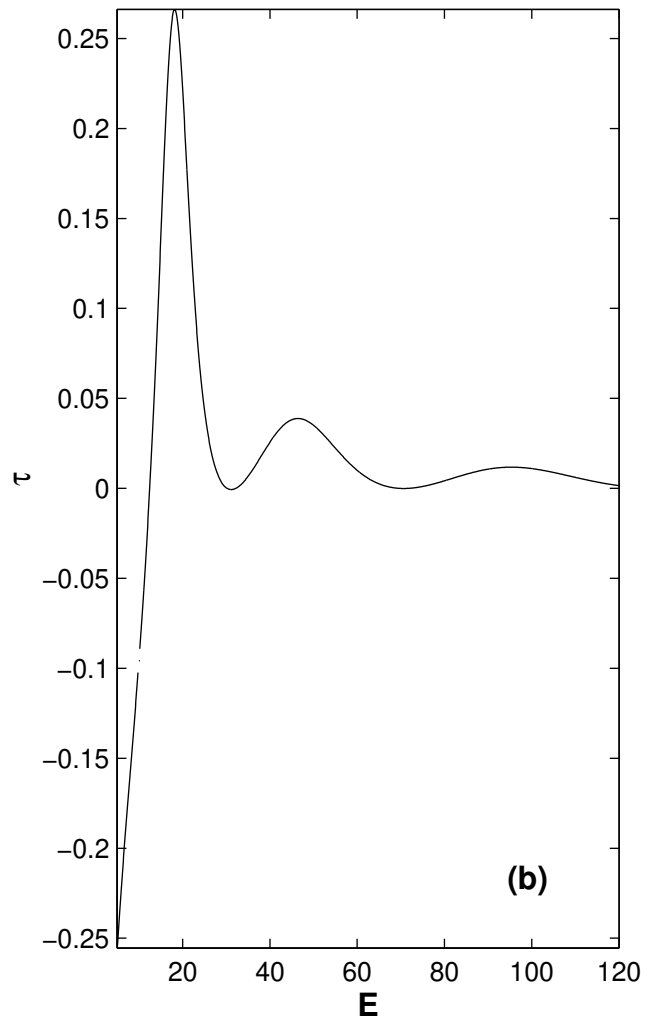
Figure 10: The normalized probability distribution, $P(\tau)$, of scaled Wigner delay times, $\tau/\langle\tau\rangle$, where $\langle\tau\rangle = \dots$ is the average value of τ , taken over all 100 realizations of the random potential.

Figure 11: The normalized probability distribution, $P(\Gamma)$, of scaled Wigner delay time half widths, $\Gamma/\langle\Gamma\rangle$, where $\langle\Gamma\rangle = \dots$ is average half-width taken over all 100 realizations of the random potential.





(a)



(b)

This figure "fig3.jpg" is available in "jpg" format from:

<http://arxiv.org/ps/nlin/0012060v1>

This figure "fig4.jpg" is available in "jpg" format from:

<http://arxiv.org/ps/nlin/0012060v1>

Fig.5, L.E. Reichl and G. Akguc

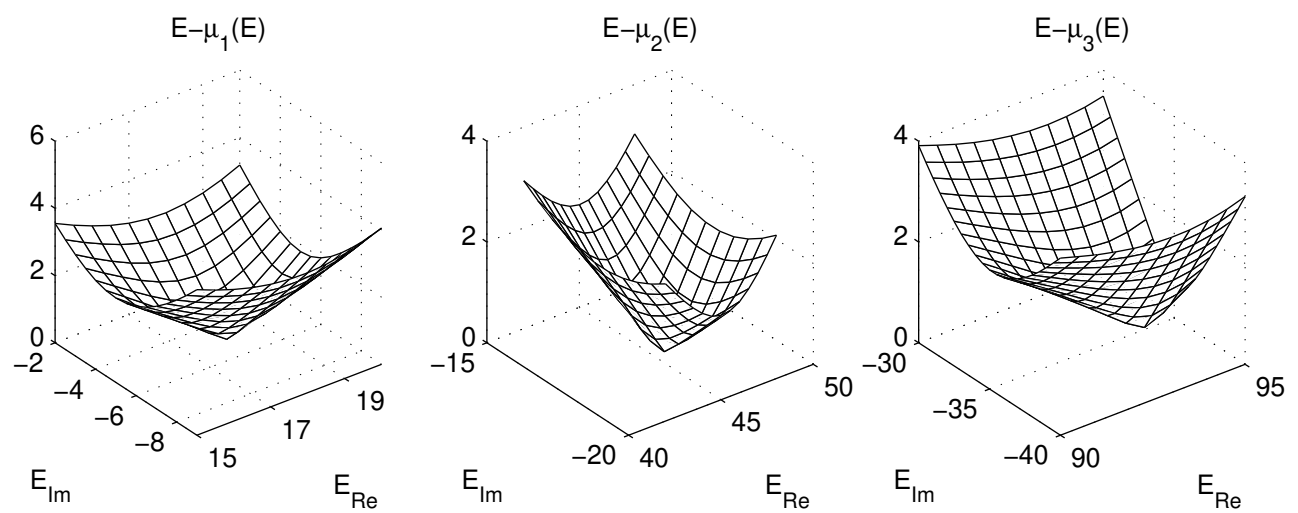
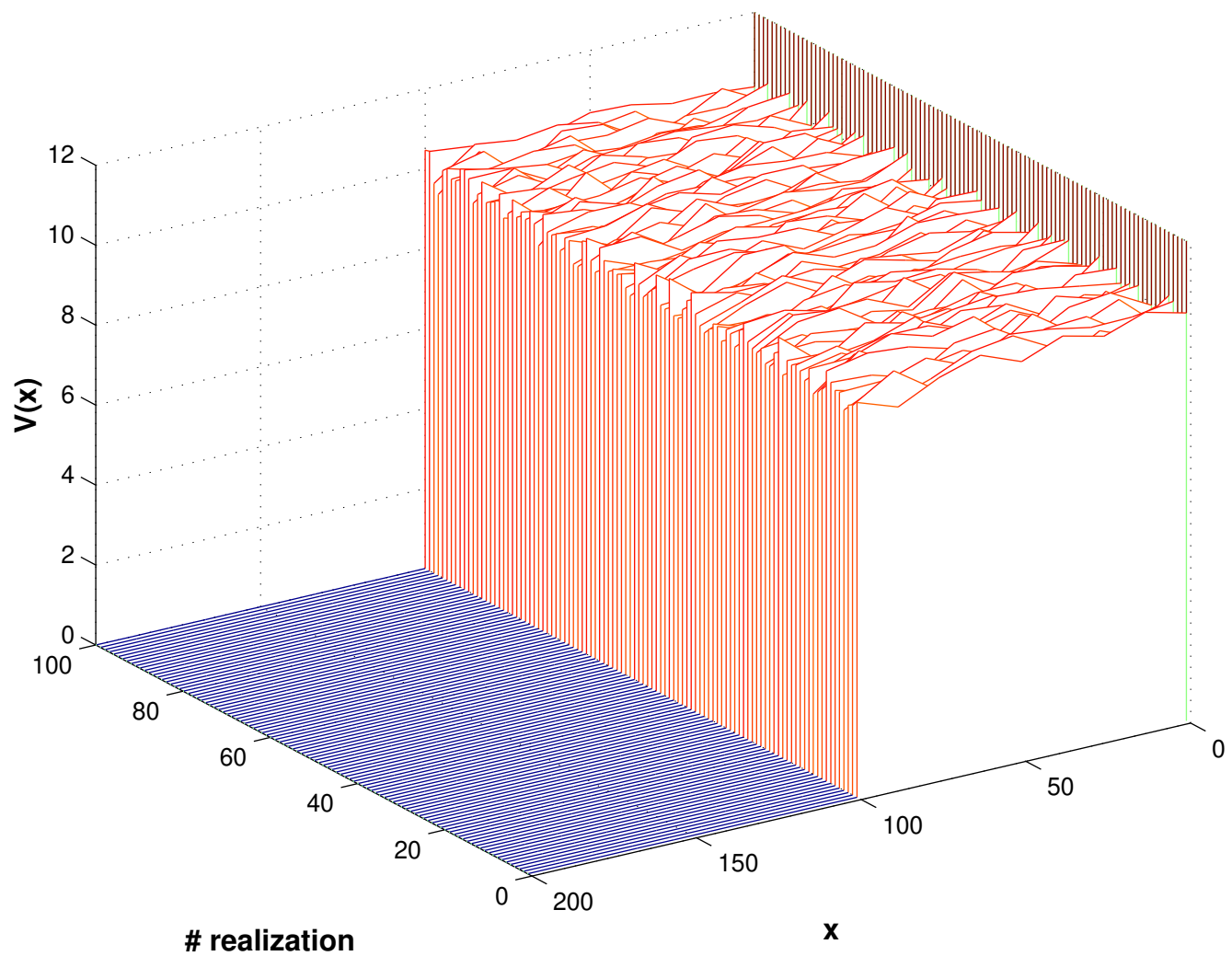
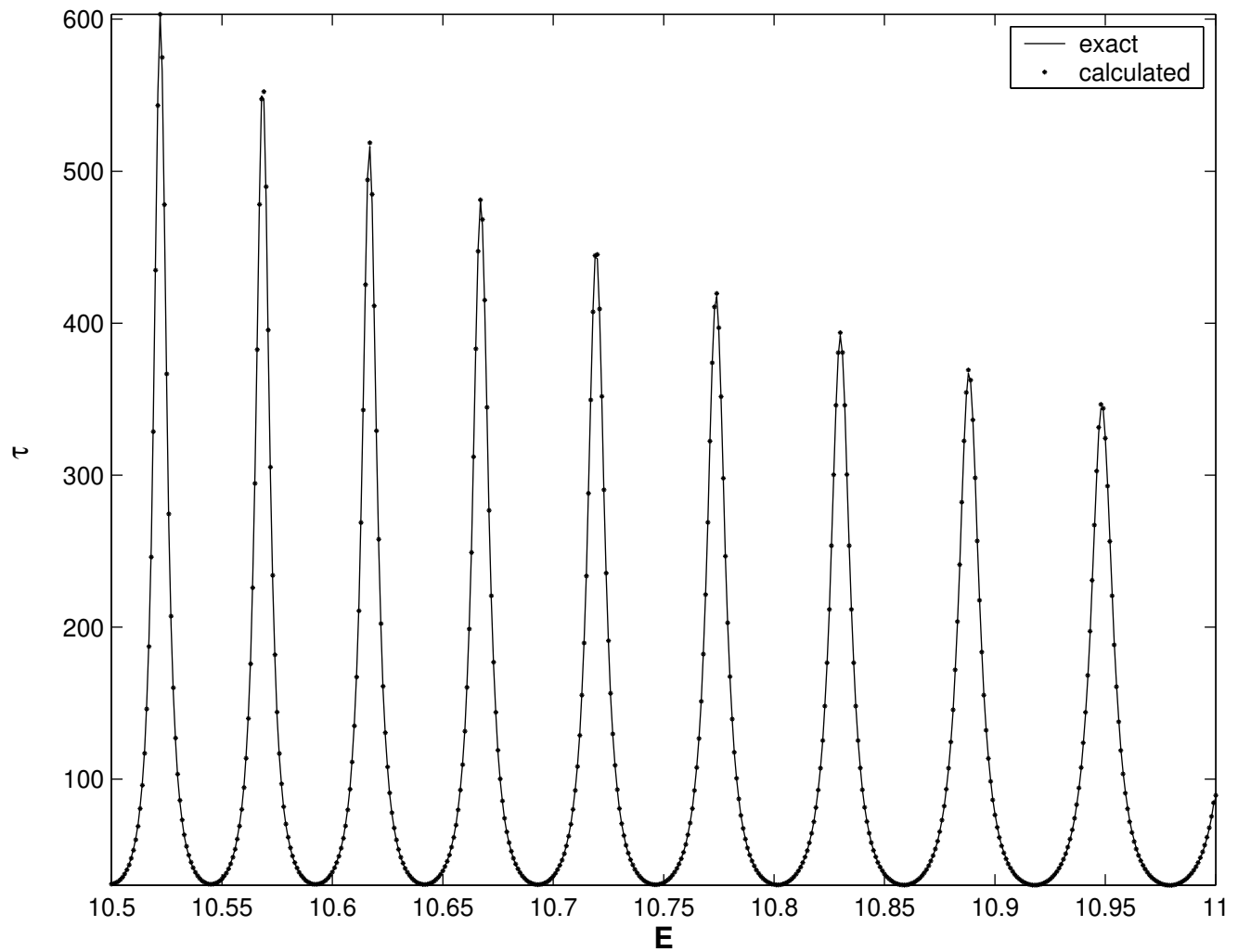


Figure 6. L.E. Reichl and G. Akguc



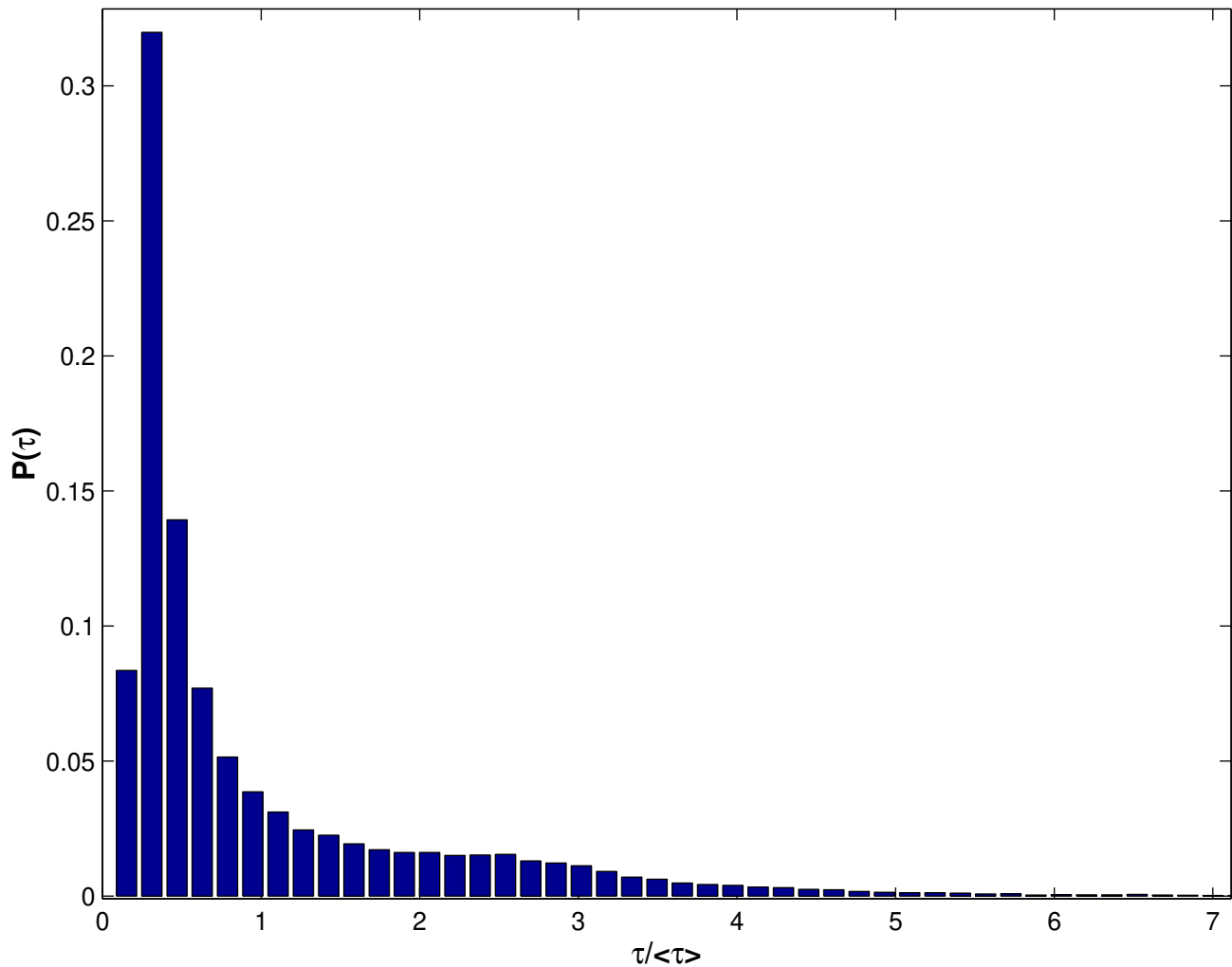
This figure "fig7.jpg" is available in "jpg" format from:

<http://arxiv.org/ps/nlin/0012060v1>



This figure "fig9.jpg" is available in "jpg" format from:

<http://arxiv.org/ps/nlin/0012060v1>



This figure "fig11.jpg" is available in "jpg" format from:

<http://arxiv.org/ps/nlin/0012060v1>